

# CRITICAL-LAYER BEHAVIOR IN AN IMPULSIVELY-PERTURBED TURBULENT BOUNDARY LAYER

**Ian Jacobi**

Graduate Aerospace Laboratories  
California Institute of Technology  
Pasadena, California, USA 91125  
jacobi@caltech.edu

**Beverley J. McKeon**

Graduate Aerospace Laboratories  
California Institute of Technology  
Pasadena, California, USA 91125  
mckeon@caltech.edu

## ABSTRACT

A zero pressure-gradient flat plate boundary layer was perturbed dynamically with a short strip of roughness, introducing large-scale velocity fluctuations in a spatially impulsive way. The velocity field was measured downstream by hot-wire anemometry, and the subsequent velocity fields were analyzed spectrally. Composite spectral maps of the distribution of streamwise turbulent energy revealed that the motions induced in the flow by the perturbation were coherent over a significant downstream area. The velocity signals were decomposed in a phase-locked sense and the modes of velocity fluctuation were described. The relative phase between the forced velocity oscillations and the turbulent fluctuations was studied by considering a mean period of the phase-locked velocity signals. This phase-relationship between forced, large-scale (singular) structures and the remaining unforced scales in the flow was compared with the work of Mathis *et al.* (2009) and Chung & McKeon (2010) on the amplitude modulation of small scales by large scale structures in unforced turbulent shear flow. The ‘active roughness’ wall actuation was shown to alter the scale modulation observed in the flow, and the differences between the two approaches to observing this modulation provide a new way of thinking about the significance of the correlation between large and small scales and the physical interpretation of skewness in turbulent flows.

## BACKGROUND

Recent interest in the decomposition of turbulent shear flows, whether by means of standard POD analysis, shown recently in Hellström & Smits (2011), or using a singular mode resolvent approach, outlined in McKeon & Sharma (2010), has demonstrated that certain significant features of turbulent flows can be described by just a few dominant modes of velocity fluctuations. One of the questions precipitated by this work is the relationship between these dominant modes and

less dominant modes – in particular, the modulating effect of dominant modes on small scales in the flow. Mathis *et al.* (2009) experimentally explored the question of the modulation of small scales by larger scales by considering a correlation coefficient  $R_\tau$  which represented the correlation between the filtered envelope of small-scale fluctuations with large scale fluctuations. Chung & McKeon (2010) employed a similar technique in a computational study of channel flow, as did Guala *et al.* (2011) in the atmospheric surface layer. The former two studies found that this measure of scale-modulation produces a distinctive shape across the half-height of the channel (or pipe radius or boundary layer). Mathis *et al.* (2009) observed that this distinct shape of the correlation profile was remarkably similar to the profile of the streamwise skewness across the boundary layer (where skewness is defined as the third moment of streamwise velocity fluctuations normalized by the three-halves power of the second moment); subsequently Schlatter & Örlü (2010) demonstrated that this similarity was not merely accidental, but in fact appeared to be a consequence of the method of calculation of the correlation coefficient itself. Whatever the mathematical similarity between the correlation coefficient and the skewness, the question remains, what is the appropriate interpretation of the skewness in the context of large-scale to small-scale modulation in turbulent flows? Mathis *et al.* (2009) observed that the wall-normal location of the zero-crossing of  $R_\tau$  overlapped the location of the outer peak in the streamwise energy spectrum and further established a direct and negative association between zero-crossing position (in outer-scaling) and Reynolds number – both of which indicate structural significance to the shape of the  $R_\tau$  and skewness profiles. The current study offers a different perspective on this question, by considering a turbulent boundary layer with periodic forcing applied by means of a short strip of oscillating roughness elements. By forcing the flow periodically, a phase-locked decomposition of the flow can be considered, similar

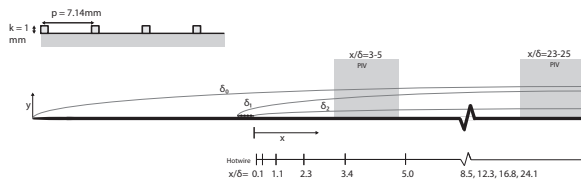


Figure 1. A schematic of the arrangement of the flat plate, the roughness strip, and the diagnostic locations; not to scale. The internal layers are also marked in order to provide an idea of the relative size and development rates.

to earlier studies of vibrating ribbons performed by Hussain & Reynolds (1970), but the dominance of the external forcing in the current experiments allows for new insights into the relationship between the large and small scale motions in the turbulent flow. Guala *et al.* (2011)

### DYNAMIC PERTURBATION EXPERIMENT

A zero pressure gradient turbulent boundary layer was explored over a flat plate in the  $2' \times 2'$  wind tunnel at Caltech. The boundary layer was tripped by a cylindrical wire just downstream of the elliptical leading edge, and the virtual origin of the turbulent boundary layer was measured 0.22m downstream of the leading edge. Approximately 1m downstream of the leading edge, the flat plate was modified to allow an array of two-dimensional roughness elements, fixed on a single patch, to pass through grooves in the plate, as diagrammed in figure 1. The elements could be fixed in at a single amplitude as a ‘static’ spatially-impulsive patch of roughness, described in Jacobi & McKeon (2011*b*); or the patch could be actuated mechanically by a motor and crankshaft assembly, in order to alternate the amplitude of the roughness elements sinusoidally, from a condition flush with the surface of the flat plate, to a maximum amplitude matched to the static case (such that the root-mean-square amplitude of the dynamic perturbation is equal to the static amplitude), as described in Jacobi & McKeon (2011*a*). During this ‘dynamic’ roughness perturbation, the phase of the roughness was measured by a magnetic linear encoder, with spatial resolution of  $1\mu\text{m}$ . The phase of the roughness perturbation was synchronized with the hotwire measurements of the downstream flow field, in order to allow for phase-locked decomposition of the instantaneous velocity time series. Hotwire measurements were recorded at 11 logarithmically-spaced streamwise locations, at 27 logarithmically-spaced wall-normal locations. In addition, PIV measurements in the streamwise-wall-normal plane were recorded at two downstream locations.

### SPECTRAL COMPOSITE MAPS

Following the approach of Hutchins & Marusic (2007), the spectral composite maps of the streamwise turbulent fluctuations were calculated from the velocity time signals, transforming the frequency domain using Taylor’s hypothesis (with the local mean convective velocity) into a wavelength domain. The maps corresponding to the unperturbed flow and the statically perturbed flow are shown in figure 2. The statically perturbed case is provided for comparison with the dynamically

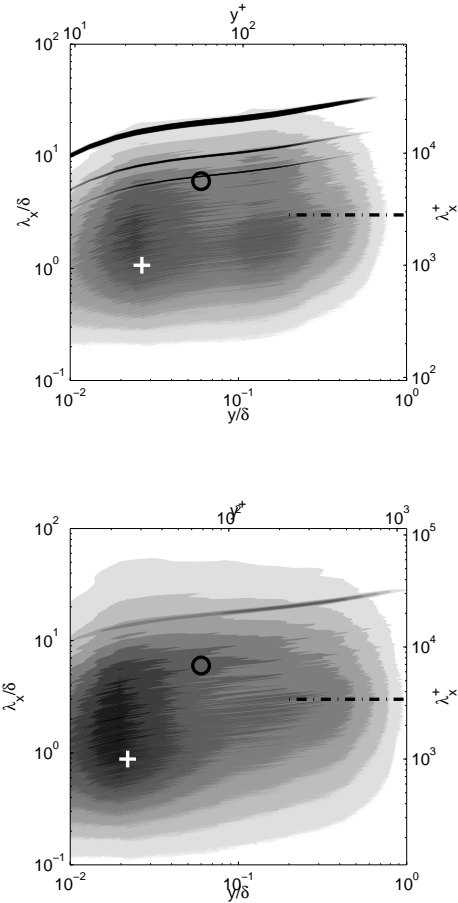


Figure 3. (Top) Composite spectra for the perturbed case at  $x/\delta = 2.3$ ; levels follow figure 2 and are the same as in Jacobi & McKeon (2011*b*) (Bottom)  $x/\delta = 23.7$

perturbed flows, shown in figure 3. Both the static and dynamically perturbed flows show a displacement of spectral energy away from the wall – an expected consequence of the two-dimensional elements – as well as a noticeable suppression of the near-wall cycle in the immediate vicinity of the perturbation. Moving farther downstream, the near wall cycle quickly recovers and the displaced energy slowly dissipates. The significant feature of the dynamically perturbed flow, however, is the presence of the signature of the dynamic forcing and its harmonics. This spectral signature tends to extend through most of the boundary layer and over a significant streamwise extent, indicating that the forcing produces a coherent and persistent modification of the boundary layer even far from downstream ( $> 20\delta$ ). And in particular, the forced motions are large-amplitude motions, with wavelength on the upper end of the spectrum of wavelengths associated with large-scale and very-large scale motions.

The coherent nature of the perturbation indicates the usefulness of a phase-locked decomposition of the instantaneous velocity field, in order to identify the shapes of large-scale velocity fluctuation produced in the flow and their relationship to the smaller scales.

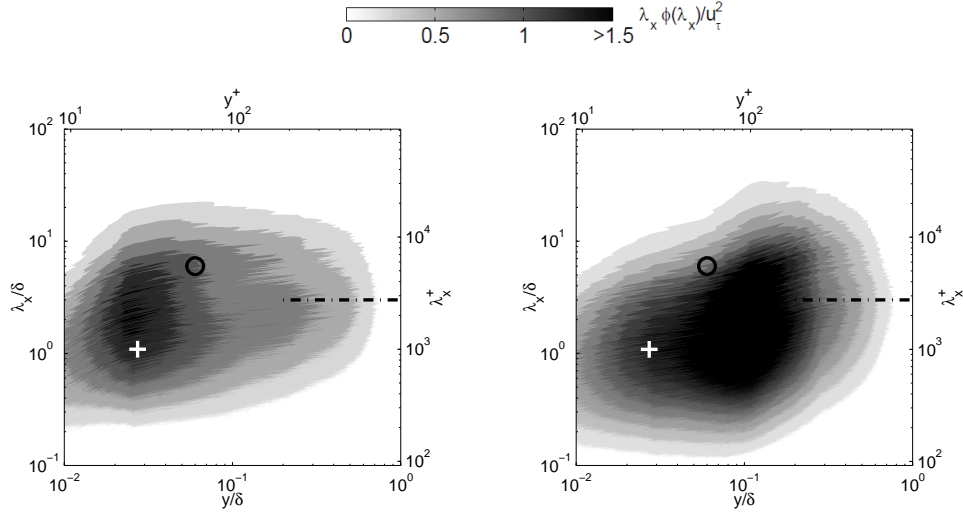


Figure 2. Composite spectra at  $x/\delta = 0.6$ : (Left) Unperturbed  $Re_\theta = 2770$  The white '+' marks the vicinity of the inner peak ( $\lambda_x^+ \approx 1000, y^+ \approx 25$ ), the black  $\circ$  marks the expected location of the VLSM peak at  $(\lambda_x/\delta \approx 6)$ , and  $\cdots$  marks the peak along  $\lambda_x/\delta \approx 3$ ; (Right) Statically perturbed, with markings as in the left plot.

## PHASELOCKED VELOCITY MEASUREMENTS

Following the velocity decomposition proposed by Hussain & Reynolds (1970), the instantaneous velocity signal  $u(y, t)$  can be decomposed into a temporal mean  $U(y)$ , a component phase-locked to the dynamic perturbation  $\tilde{u}(y, t)$  (which has, by definition, zero mean), and a remaining fluctuation quantity,  $u'(y, t)$ . The same decomposition was performed for the wall-normal velocity signal  $v(y, t)$ , although the remainder of this paper will treat only the streamwise velocity components.

$$u(y, t) = U(y) + \tilde{u}(y, t) + u'(y, t) \quad (1)$$

The remainder of the analysis will consider these quantities ensemble-averaged over each phase, in order to consider a 'mean period' of the velocity fluctuations in the flow. Therefore, for the remainder of the paper, the quantity  $u'(y, t)$  will be taken to refer to the root mean square value of the fluctuations as opposed to the actual mean fluctuations, which are zero in the ensemble averaged sense.

The relative energetic content in the different components of the velocity are of interest. One measure of the energy content can be formulated as the ratio of the integrated kinetic energy of the disturbances across the boundary layer, given by equation 2

$$Er(u_i, u_j) = \frac{\int_0^\delta u_i dy}{\int_0^\delta u_j dy} \quad (2)$$

where  $u_i$  and  $u_j$  represent components of the phase-locked decomposition given in equation 1. The ratios of the different components are tabulated with the ratio given as the column

value over the row value in table 1. Note that the two replicated values between the hotwire and PIV values are consistent with an error of less than 10%.

Table 1. Integrated fluctuating intensities,  $Er(u_{col}, u_{row})$

	$\tilde{u}_{HW}$	$\tilde{u}$	$\tilde{v}$	$u'$
$u'_{HW}$	<b>11.58</b>			
$\tilde{v}$		7.64		
$u'$		<b>12.55</b>	1.64	
$v'$		25.59	3.35	2.04

The integrated fluctuating energy in the streamwise direction  $u'$  is roughly twice that of the wall normal direction,  $v'$ , while the phase-locked component is almost eight times larger. As discussed in Jacobi & McKeon (2011a), these ratios are not expected to remain constant downstream of the perturbation, as the 'internal forcing' of the shear flow (i.e. the non-linearities of the flow, as described in McKeon & Sharma (2010)), expressed in the Reynolds normal stresses, are not isotropic, and therefore the relative rates of decay of the phase-locked signals in the streamwise and wall-normal directions are expected to be significantly different. But at least locally at one streamwise location, these ratios provide a sense of the relative strength between large and small scales and thus provide a context for interpreting the subsequent phase analysis. They also demonstrate that the forcing involved in the current study, using a patch of dynamically actuated roughness elements, is significantly stronger than that obtainable by the vibrating ribbon used in past studies, as de-

scribed in Jacobi & McKeon (2011a).

## PHASE DIFFERENCES

In order to consider the relationship between the large-scales and small-scales in the flow, Mathis *et al.* (2009) proposed defining a correlation coefficient relating the envelope of small-scale motions, identified by means of a Hilbert transform of a high-pass filtered velocity signal, and the corresponding low-pass velocity signal. Chung & McKeon (2010) noted that this correlation coefficient  $R_\tau$  is equivalent to the inner-product of these two signals and thus conveys information about the phase-difference  $\phi$  between the large and small-scale motions, according to the standard relationship for inner-products,  $R_\tau = \cos \phi$ .

Both of the approaches of Mathis *et al.* (2009) and Chung & McKeon (2010) involve filtering the velocity signals in order to separate the different scale sizes before constructing the correlation coefficient. The phase-locked velocity signals of the current study provide a different means of directly measuring the relationship between the phase-locked (large scale) forcing,  $\bar{u}$ , and the envelope of fluctuations,  $u'$ , by considering the mean period of these quantities, ensemble averaged over all phases. From the mean periods of these two quantities, the relative phase between each velocity component  $\phi_p$ , as a function of wall-normal location, can be identified from a cross-correlation of the two signals. And then the cosine of this phase-difference can be represented as  $R_p = \cos \phi_p$ , in order to distinguish this quantity, which represents the phase between the single, dominant large scale and remaining scales, from  $R_\tau$  which represents the phase difference between an integrated average of large scales (via the filtering) and smaller scales. Both of these methods will be examined below.

Consider first a map of  $\bar{u}$  over an average period at a given streamwise location, in figure 4a. The positive and negative fluctuations form a distinctive mode shape, characterized by a reasonably sharp inclination in the streamwise direction near the wall; an amplitude maximum around  $y/\delta \approx 0.1$ ; and a phase-shift in the wall-normal direction of  $180^\circ$  farther from the wall. These three characteristics are typical of the critical layer velocity modes familiar from solutions of the Orr-Sommerfeld problem, and detailed in McKeon & Sharma (2010). These velocity modes represent the single large-scale modulating wave in the flow – its dominance was apparent from the spectral composite maps shown above, in figure 3.

The envelope of the fluctuations (as represented by the root mean square amplitude of the fluctuations) is shown in figure 4b. The shape of these fluctuating modes shares some similarity with the large-scale, forced modes; in particular, the inclination of the modes and the peak amplitude near the wall. However, the smaller-scales appear to be exactly out of phase with the forced scales over a significant fraction of the boundary layer. For comparison, the contour lines (representing 1% deviation from both the positive and negative side of zero) from the small-scale modes are superposed on the contour regions of the large-scale fluctuations, in figure 4a. It is quite apparent that very near the wall and far away from the wall (past the  $180^\circ$  phase shift in the large scale modes), the small and large scales are again in phase.

By calculating the phase difference between the dominant scale of the forcing and the fluctuating scales in the flow, ex-

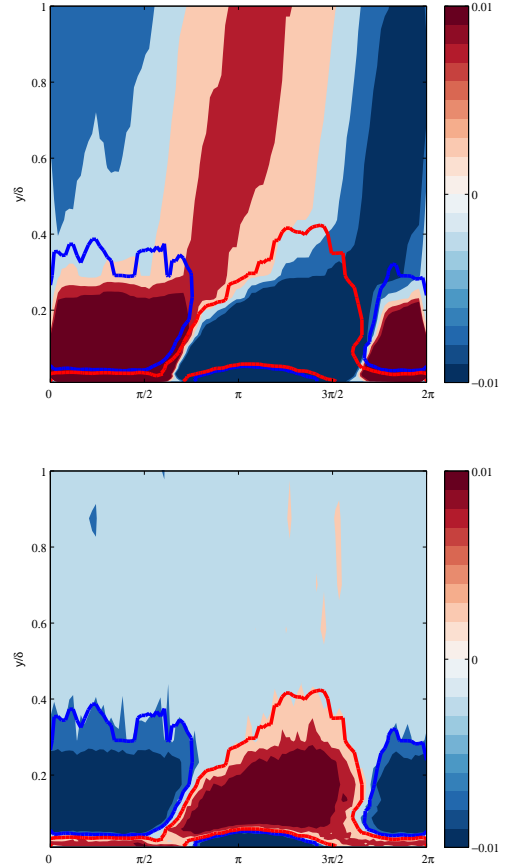


Figure 4. The maps for the streamwise velocity components. Top:  $\bar{u}$ ; Bottom: the envelope of the root mean square amplitude fluctuations of  $u'$ . All measurements are taken at  $x/\delta \approx 0.3$  in order to capture the undistorted mode shapes; farther downstream the modes tend to spread in the wall-normal direction.

pressed as  $R_p$ , the change in relative phase across the boundary layer is seen to evolve moving downstream, away from the initial perturbation, as shown in figure 5. The key features observed above are apparent again: the different scales are in phase near the wall, almost exactly out of phase out until the location of the  $180^\circ$  phase shift in the large scales, and then are in phase again, outside the mean edge of the boundary layer. Mathis *et al.* (2009) also observed this return to in phase alignment outside the mean edge of the boundary layer, although the correlation dropped rapidly to zero farther away from the wall. The zero-crossing of the phase, which represents the wall-normal location at which the large and small scales are out of phase by  $90^\circ$ , varies as a function of streamwise measurement location. The significance of this zero-crossing suggested in Chung & McKeon (2010) is that it represents the shift from in phase to out of phase alignment of small and large scales that occurs as a result of a chain of inclined, alternating high and low speed regions of large scale motion in the flow.

Returning to the definition of  $R_\tau$  offered in Chung & McK-

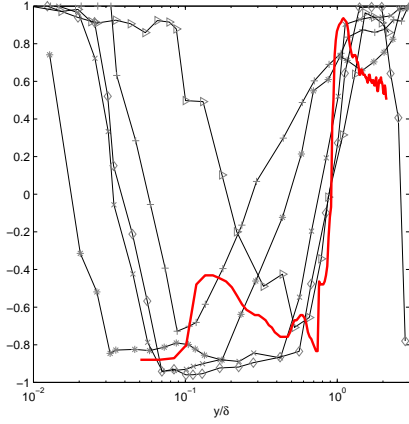


Figure 5. Phase differences represented as  $R_P$  between  $\tilde{u}$  and the envelope of  $u'$  across the boundary layer: — from PIV; hotwire measurements at  $x/\delta = 0.1 +$ ;  $0.6 *$ ;  $2.3 \times$ ;  $5.0 \diamond$ ;  $12.1 \nabla$ .

eon (2010), the correlation coefficient can be calculated by appropriate filtering of the velocity time series (using a tapered-window on the entire time series, without phase-locking) and then cross-correlating the two quantities representing the large scales,  $u_L$ , and small scales,  $\tilde{u}_s$ , represented in equation 3.

$$R_\tau = \frac{\langle (u_L - U(y))(\tilde{u}_s - \langle \tilde{u}_s \rangle) \rangle}{\langle (u_L - U(y))^2 \rangle^{1/2} \langle (\tilde{u}_s - \langle \tilde{u}_s \rangle)^2 \rangle^{1/2}} \quad (3)$$

This formulation will necessarily include a diversity of larger scales found in the flow, determined by the width of the taper (a set number of eddy-turnover times  $\tau \sim \delta/U_\infty$ ), and not merely the single dominant scale applied to the flow, examined above with phase-locking. In addition to the calculation of  $R_\tau$ , the skewness of the streamwise turbulent fluctuations can also be calculated for comparison with the correlation coefficient, following the observation of Mathis *et al.* (2009).

Although there is some variation with choice of taper width  $\tau$ , the shape is relatively robust for  $\tau U_\infty/\delta = 1 - 20$ , as found in Chung & McKeon (2010). Choosing an intermediate value  $\tau U_\infty/\delta = 5$  produced a series of profiles which overlap almost exactly with the skewness profiles calculated for the identical time series. The only significant differences occurred near the mean edge of the boundary layer and can most likely be attributed to intermittency effects. Importantly, the profiles of  $R_\tau$  share the same three characteristic features as those for  $R_P$ , namely: the large and small scales are in phase near the wall, then out of phase for a significant fraction of the boundary layer, and finally in phase again far from the wall. And again the zero-crossing appears to vary as a function of streamwise distance downstream of the perturbation.

The differences between these two measures of the large-scale modulation of smaller scales appear in the width and magnitude of the out of phase region of the boundary layer, and the wall-normal location of the zero-crossing. The correlation coefficient based on only the dominant scale,  $R_P$ , shows

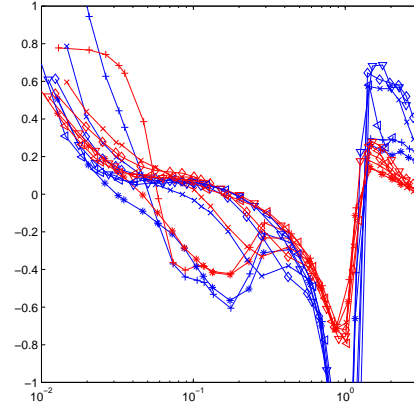


Figure 6. Following the approach of Chung & McKeon (2010): Skewness,  $R_\tau$  Symbols as in figure 5

a significantly broader region of the boundary layer where the fluctuations are almost identically out of phase, while the skewness and  $R_\tau$  show a narrower region, in which the phase shift is closer to  $60^\circ$  out of phase. And the zero-crossing for  $R_P$  tends to occur further from the wall than that of  $R_\tau$ , at least within  $15\delta$  of the perturbation; far downstream the two values appear roughly the same, consistent with the relaxation of the perturbed flow, as described in Jacobi & McKeon (2011a). To better compare the trend in the zero-crossing, the zero-crossing locations for the three measures are shown as a function of streamwise position in figure 7. The zero-crossing of  $R_\tau$  tends to increase, moving downstream, until around  $10\delta$ , after which it decreases and then attains a roughly constant value for the last two streamwise location; this trend is match by the skewness zero-crossing. For  $R_P$ , the zero-crossing initially appears to attain the far downstream value (around  $y/\delta = 0.2$ ), but it quickly drops off and then slowly recovers going downstream, until around  $15\delta$ , at which point it stabilizes near to the value found by  $R_\tau$ .

Besides the interpretation of the zero-crossing ( $90^\circ$  phase difference) as relating to the sequence of low and high speed velocity fluctuations in an inclined orientation, the zero-crossing locations obtained in Örlü (2009) and Mathis *et al.* (2009) are also observed to overlap the location of the outer peak in the streamwire energy spectrum, and, in turn, indicate a direct and negative association between zero-crossing position (in outer-scaling) and Reynolds number. Therefore, the case of the dynamic perturbation is observed to cause a decrease in the zero-crossing of  $R_\tau$  immediately downstream of the perturbation, followed by an overshoot in the recovery, which perhaps can be interpreted as a local appearance of higher Reynolds number behavior driven by the forcing and associated alteration of the structure of the flow. In the case of  $R_P$ , the decrease in zero-crossing position persists for much longer, with a monotonic recovery.

The question is what explains the differences between the two measures of large to small scale correlation – in particular the shift of the zero-crossing closer to the wall in the case of  $R_P$  and the differences in the recovery? From the geometrical picture in Chung & McKeon (2010), the shift nearer to the

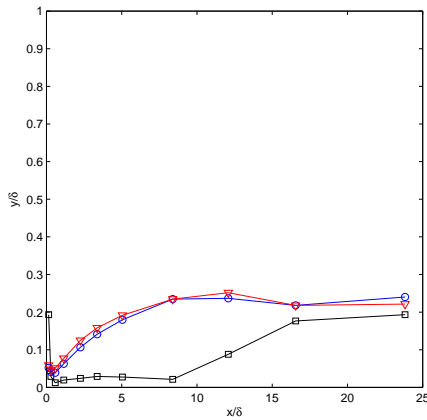


Figure 7. The wall-normal location of zero-crossing as a function of streamwise position downstream of the perturbation.  $\circ$  for skewness profiles;  $\nabla$  for  $R_\tau$ ;  $\square$  for  $R_p$

wall can be interpreted as a change in the mean inclination angle of the large structures (which fixes the point at which the phase is  $90^\circ$  out of phase) or the small-scale envelope, which would indicate that the inclination of the forced modes is different from the average of all of the larger scale modes. To investigate the difference among the forced and unforced large scales, we can look at the phase between a band-pass filtered signal at approximately the forcing frequency and the same low-pass filter used for the large scales,  $u_L$ . If the band about the forcing frequency behaved the same as the average of the large scales, then the signals would appear highly correlated, with negligible phase-difference. However, there appears to be significant variation in the phase-relation between the two means of describing the large scales in the forced flow, indicating that average of the large scales captured in  $u_L$  is not equivalent to considering just the forced large scale. Similar investigations are currently being applied to the small-scale and fluctuating envelopes. In any case, the structural (inclination angle) differences are observed to relate directly to the shape of the correlation profile, which may have implications for the physical interpretation of the skewness profiles.

## DISCUSSION AND CONCLUSIONS

The dynamic perturbation of a flat plate turbulent boundary layer induced large-scale velocity modes with a distinctive shape. The envelope of turbulent fluctuations about these phase-mean mode shapes also produced a distinctive shape, which enabled identification of the relationship between forced large and small scales. The overlap of these two mode shapes revealed that the relative inclination of small and large scale motions has significant importance to the relative phase between the structures, as noted by Chung & McKeon (2010). This relative phase was investigated by comparing the mean periods of these two velocity components (large and small scales), and using cross-correlations to identify the phase-difference between the modes as a function of wall-normal position in the boundary layer. This phase relation,  $R_p$ , was compared with the correlation coefficient used by

Mathis *et al.* (2009) and Chung & McKeon (2010) to measure the amplitude modulation of small scales by large scales in unforced turbulent flows,  $R_\tau$ , which in turn appears to be related to the skewness of the streamwise velocity fluctuations. The latter correlation coefficient reflects the relation between the envelope of the amplitude of the small scales to an average set of the large scales, while the former measure reflects the relation between the envelope of fluctuations and just one large scale, namely the forcing. These two correlation measures shared significant features in common, in particular: correlation near the wall, a zero-crossing, and then negative correlation out through the intermittent edge of the boundary layer. However, the shape of the phase variation across the boundary layer did differ between the two measures, and that difference was suggested to stem from structural differences between the forcing velocity modes and the mean of the large scales including those modes. Under the conceptual picture introduced in Chung & McKeon (2010), that difference could be interpreted as related to the relative inclination of different sized structures in the flow field.

This work is supported by the Air Force Office of Scientific Research Hypersonics and Turbulence portfolio, under grant #FA9550-08-1-0049 (Program Manager John Schmisser).

## REFERENCES

- Chung, D. & McKeon, B.J. 2010 Large eddy simulation of large scale structures in long channel flow. *Journal of Fluid Mechanics* **661**, 341–364.
- Guala, M., Metzger, M. & McKeon, B.J. 2011 Interactions across the turbulent boundary layer at high Reynolds number. *Journal of Fluid Mechanics* **666**, 573–604.
- Hellström, L.H.O. & Smits, A.J. 2011 Visualizing the very-large-scale motions in turbulent pipe flow. *Physics of Fluids* **23**.
- Hussain, A.K.M.F. & Reynolds, W.C. 1970 The mechanics of an organized wave in turbulent shear flow. *Journal of Fluid Mechanics* **41**, 241–258.
- Hutchins, N. & Marusic, I. 2007 Large-scale influences in near-wall turbulence. *Philosophical Transactions of the Royal Society* **365**, 647–664.
- Jacobi, I. & McKeon, B.J. 2011a Dynamic roughness-perturbation of a turbulent boundary layer and the excitation of ‘critical layer’ velocity modes. (*submitted*).
- Jacobi, I. & McKeon, B.J. 2011b New perspectives on the impulsive roughness-perturbation of a turbulent boundary layer. *Journal of Fluid Mechanics* (*to appear*).
- Mathis, R., Hutchins, N. & Marusic, I. 2009 Large-scale amplitude modulation of the small-scale structures in turbulent boundary layers. *Journal of Fluid Mechanics* **628**, 311–337.
- McKeon, B.J. & Sharma, A.S. 2010 A critical layer model for turbulent pipe flow. *Journal of Fluid Mechanics* **658**, 336–382.
- Örlü, R. 2009 Experimental studies in jet flows and zero pressure-gradient turbulent boundary layers. PhD thesis, Royal Institute of Technology.
- Schlatter, P. & Örlü, R. 2010 Quantifying the interaction between large and small scales in wall-bounded turbulent flows: A note of caution. *Physics of Fluids* **22**.